

See discussions, stats, and author profiles for this publication at: <https://www.researchgate.net/publication/231667438>

Assessing the Solution Shape and Size of Charged Dendronized Polymers Using Double Electron–Electron Resonance

ARTICLE *in* JOURNAL OF PHYSICAL CHEMISTRY LETTERS · JUNE 2011

Impact Factor: 7.46 · DOI: 10.1021/jz200653k

CITATIONS

18

READS

51

5 AUTHORS, INCLUDING:



Dennis Kurzbach

Max F. Perutz Laboratories

24 PUBLICATIONS 138 CITATIONS

SEE PROFILE



Baozhong Zhang

Lund University

29 PUBLICATIONS 379 CITATIONS

SEE PROFILE



Dariush Hinderberger

Martin Luther University Halle-Wittenberg

106 PUBLICATIONS 1,050 CITATIONS

SEE PROFILE

Assessing the Solution Shape and Size of Charged Dendronized Polymers Using Double Electron–Electron Resonance

Dennis Kurzbach,^{†,§} Daniel R. Kattnig,^{†,§} Baozhong Zhang,[‡] A. Dieter Schlüter,[‡] and Dariush Hinderberger^{*,†}

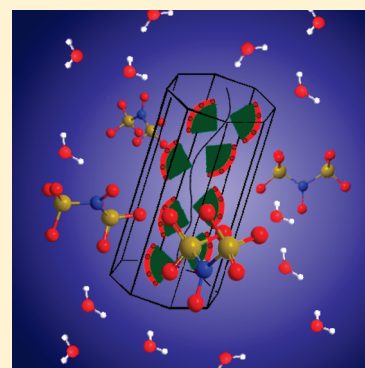
[†]Max Planck Institute for Polymer Research, Ackermannweg 10, 55128 Mainz, Germany

[‡]Department of Materials, Institute of Polymers, ETH Zurich, Wolfgang-Pauli-Str. 10, Zurich 8093, Switzerland

S Supporting Information

ABSTRACT: We present double electron–electron resonance (DEER) data that suggest that highly branched dendronized polymers (denpols) in solution are macromolecules with persistent shape, a well-defined envelope, and a size independent of their environment. By determining the distance distribution of self-assembled dianionic spin probes (Fremy's salt dianion) on the surface of the cylindrically shaped and cationic denpols, we show that the measured solution radii are in good agreement with the solid-state radii of the neutral denpol analogues. An analytic distance distribution of particles on the lateral surface of cylinders is developed for this purpose and fitted to DEER time traces. Such, DEER in combination with site-directed spin probing provides an indirect and simple method to determine the solution shape and size of macromolecules on the nanometer scale. It furthermore shows that at least generation four and three denpols in solution may already be described as molecular objects.

SECTION: Macromolecules, Soft Matter



This Letter addresses the solution structure of a class of dendronized polymers (denpols) that have attracted recent attention as potential lead structures for molecular objects. This term refers to nanostructured objects exhibiting a persistent shape, independent of their immediate environment, and having a well-defined envelope.¹ Molecular objects are in the spotlight of an emerging, ambitious discipline of chemical synthesis that focuses on forming the overall shape of mesostructures. For molecular objects, the solution structure is obliged to not differ significantly from its solid-state structure. For most macromolecules, even biomacromolecules, a striking difference between liquid- and solid-state structures is observed. We have, for example, recently shown by double electron–electron resonance (DEER) spectroscopy that even for the well-folded protein human serum albumin (HSA) the solution structure differs significantly from the crystal structure.² There, we found that the entry points of fatty acids into HSA are distributed highly symmetrical over the surface of the protein in solution to optimize fatty acid uptake, whereas an asymmetric distribution can be observed in the crystal structure.

Among other advantages, denpols have tunable thicknesses and high persistence lengths.³ From the structural point of view, they are linear polymers, whose repeat units all carry dendrons of variable generation (the number of branching units, n ; here, the number of terminal groups is 2^n) and termination (the end groups of the outer shell).^{1b,4} The denpols studied here are based on poly(methacrylate) and carry positively charged ammonium groups at their peripheral end groups (cf. Figure 1, Figure S2 in the Supporting Information). The densely packed dendrons around the backbone render the polymer's shape cylindrical and provide

it with variable stiffness and diameter.⁵ Recently, a generation five species has been reported that can be considered to be a molecular object because of its considerable stiffness (persistence length $l_p \approx 30$ nm) and the fact that it largely maintains its cross-section geometry when deposited on a solid substrate.^{1b}

To study the shape and size of dendronized polymers in solution, we apply DEER spectroscopy, an electron paramagnetic resonance (EPR) technique measuring the dipolar coupling frequency of two or more electron spins, which itself depends on the interspin distance r .⁶ In practice, distance distributions ranging from approximately 1.5 to 8 nm can be obtained. (For experimental details, see the Supporting Information.)⁷

Here we show that DEER is suitable to determine the size (thickness) of different generations of cylindrical denpols in solution. The claim that any conventional polymer is rendered into a molecular object by attaching high-generation dendrons to each of its main chain repeat units is substantiated by showing that the difference between the solid-state radius and the solution size decreases with growing generation. Furthermore, we show that the DEER-based characterization of dianionic spin probes that self-assemble close to the surface of cationic denpols is an indirect and yet precise method to determine the effective spatial constitution and diameter of large, charged objects in solution.

To determine distance distributions by DEER spectroscopy, spin labels are usually covalently bound to well-defined positions of a molecule (e.g., a protein).⁸ Whereas this spin labeling

Received: May 14, 2011

Accepted: June 8, 2011

Published: June 08, 2011

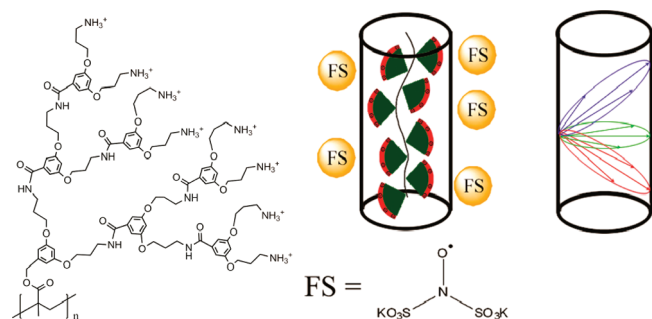


Figure 1. Molecular structure of de-PG3 with the peripheral ammonium groups is shown on the left. In the center, the coordination of FS on the cylindrical surface of the dendronized polymers is shown schematically. The possible distances of a spin on the surface of a cylinder to points on the surface are sketched in the Figure on the right. The red, blue, and green ellipses represent only three of an infinite number of possible orientations.

approach is, in principle, not out of question for the denpols studied here, comparable insights can be achieved relying on the self-assembly of doubly negatively charged spin probe Fremy's salt (FS, potassium nitrosodisulfonate, see Figure 1) at the ammonium surface layer of high positive charge density. Room-temperature continuous wave (CW) EPR measurements on 2 mM solutions of Fremy's salt containing 1 wt % of denpol show that the line width and the rotational mobility, represented by the rotational correlation time, τ_c of the spin probe, increase notably compared with a pure solution of FS in water. (See Figure S1 of the Supporting Information.) As previously observed for polyelectrolytes, this suggests that the FS molecules are indeed electrostatically bound to the surface of the denpols.⁹

Hyperfine sublevel correlation spectroscopy (HYSCORE),¹⁰ which can resolve even small and overlapping hyperfine interactions between an electron spin and its surrounding magnetic nuclei,¹¹ shows that the electron spin of the FS is strongly coupled to at least one ^{14}N nucleus in the surrounding of the probe. (See the Supporting Information for details.) This suggests that a large fraction of FS is adsorbed at the ammonium surface. In CW EPR experiments, the isotropic hyperfine coupling constant a_{iso} of the nitoxide moiety of FS is a very sensitive probe for changes in the polarity/hydrophilicity of the environment. Because a_{iso} of FS in solutions with denpols was constant at a value representative for a purely aqueous environment (~ 36.7 MHz), one can assume that FS does not significantly penetrate the outermost surface of the denpols. Furthermore, it has been previously shown that FS binds transiently (contact time $< \sim 1$ ns) with only one of its sulfonate groups to polycations and that consequently characteristic line patterns appear in CW EPR spectra. Because the CW spectra recorded during this study resembles those found for polyelectrolytes,^{9,12} one can safely assume that FS binds with only one sulfonate group to dendronized polymers as well. Therefore, a structuring of the denpol surfaces due to a "bridging" effect between ammonium groups is not expected. Bridging between two different denpol chains is unlikely as well. The transient nature of the coordination of FS does not lead to a stable connection between two polymer chains.

Previous AFM studies indicate that in the solid state the diameter of the denpols PG1–4¹³ grows with increasing generation; PG-1 is ~ 0.8 nm thick and PG-4 is ~ 4 nm.^{1b,3a} Because one can assess distances between approximately 1.5 and 8 nm with

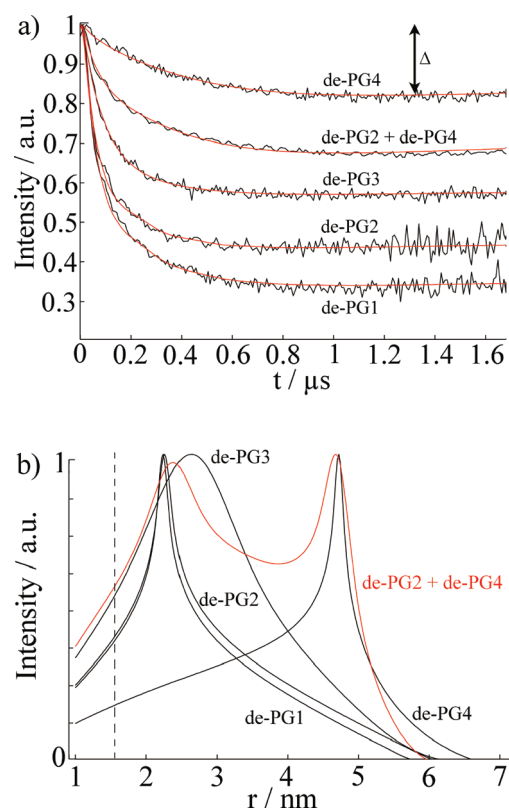


Figure 2. (a) Normalized time-traces, that is, form factors, of the dipolar evolution for FS and denpols of different generations. The red lines indicate the fits of the experimental time-traces (black lines) calculated from the assumed cylindrical distribution of Fremy's salt around the denpols. (b) Distance distributions of spins in denpol solutions containing Fremy's salt. The distributions were calculated from the fits of the experimental time-traces, presented in part a. The red line represents the bimodal distribution determined for a mixture of de-PG2 and de-PG4. The dotted line indicates the minimal observable distance, r_{min} .

DEER, one may determine the solution diameter of the denpols, which might be difficult or would involve high efforts (e.g., SANS) to access by other means.¹⁴ Figure 2a depicts the time traces of the dipolar evolution for FS ions in the presence of denpols of different generations. We also show fits (red traces) based on a physical model assuming a uniform distribution of the probes on the surface of a cylinder (described below). A very important experimentally accessible parameter is the modulation depth, Δ , of the time traces (Figure 2a), which in the linear regime depends on the number of coupled spins $\langle n \rangle$ according to¹⁵

$$\Delta = 1 - \exp(\lambda(1 - \langle n \rangle)) \quad (1)$$

λ is the so-called modulation depth factor, which essentially depends on technical parameters (excitation position, length, and flip angles of pump pulse, etc.). In Figure 2a, the number of coupled spins decreases with increasing generation, which is in line with the concurrent increase in the surface accessible to the probe (and a corresponding decrease in the surface concentration). With λ determined for the pertinent experimental settings by calibration, n has been evaluated from eq 1. Table 1 summarizes n and Δ for the investigated samples. The maximum number of coupled spins (observed for de-PG1, as could be expected)

Table 1. Radii Gained from DEER Measurements with Fremy's Salt As Spin Probe (Solution State) and from AFM Tapping Height (Solid State) Are Listed for All Generations Investigated during This Work^a

	de-PG1	de-PG2	de-PG3	de-PG4
R_{DEER} (nm)	0.8 ± 0.2^b	0.8 ± 0.2^b	1.0 ± 0.3	2.1 ± 0.4
R_{AFM} (nm)	0.2 ± 0.1	0.5 ± 0.1	1.1 ± 0.1	2.0 ± 0.4
$R_{\text{DEER}}/R_{\text{AFM}}$	4.5 ± 0.1	4.5 ± 0.1	0.9 ± 0.2	1.1 ± 0.4
Δ	0.64	0.54	0.42	0.16
n	2.41	2.07	1.75	1.24

^aRatio $R_{\text{DEER}}/R_{\text{AFM}}$ indicates the differences between the size of the denpols in the solution and solid state. Δ is the modulation depth of the DEER time-trace (cf. Figure 2a). n is the number of coupled spins (see eq 1) that determines Δ . ^bValues represent the lower distance limit of DEER.

is 2.41, which is low enough for multispin artifacts to be negligible.¹⁶

According to the shell factorization model, introduced by Jeschke et al.,¹⁷ the normalized time-domain DEER signal (Figure 2a) is related to the distance distribution, $P(r)$ (Figure 2b), by a convolution-type integral equation. (See the Supporting Information for details.) Whereas, in principle, $P(r)$ can be determined by inverting an ill-posed, inverse problem, we here assume a simple geometrical model from the outset and test it against the experimental time traces. This approach alleviates issues related to the uniqueness of the solution, which often hamper regularization approaches. (See, for example, Fajer et al. in *ESR Spectroscopy in Membrane Biophysics*¹⁸ for a discussion of advantages and drawbacks of the different methodologies.)

Given the highly constrained molecular shapes of the dendronized polymers, we shall assume that the spin probes are distributed independently and uniformly on the lateral surface of circular cylinders. Indeed, from steric considerations and the fact that the persistence lengths l_p of the neutral denpol analogues are 5–10 nm,^{1,2} de-PG1 to de-PG4 may be regarded as stretched on a length scale up to 10 nm. We have derived an analytic expression for the distance distribution $P(r)$ (cf. Supporting Information), which can be compactly expressed as

$$P(r) = \frac{2r}{L^2\pi} \left(\frac{L}{R} F(\varphi|k^2) - 2 \sin^{-1}(k \sin \varphi) \right) \bigg|_{\varphi = R \cos^{-1}(\frac{r}{R})}^{\mathcal{R} \sin^{-1}(k^{-1})} \quad (2)$$

Here F denotes the incomplete elliptical integral of the first kind. \mathcal{R} is the real part and $k = r/2R$. We work in dimensionless units with radius $R = 1$ and denote the cylinder height by L . The full development is outlined in the Supporting Information, Section C.

Fits of DEER time traces based on eq 2 yield the distance distribution of FS on the cylindrical surface formed by the dendronized polymers. (See Figure 2a.) The two essential fitting parameters are the radius (diameter) of the cylinder, R_{DEER} , and the length, L . In line with the expected persistence lengths, all values for L in the fits exceed 5 nm. This can be seen as the lower limit because it is limited by the length of the recorded time trace, indicating that on these DEER length scales denpols are essentially stiff rods. The most probable distance R_{DEER} , after correction of the finite size of the probe and its thermal motion, corresponds to the diameter of the effective cylinder and, hence,

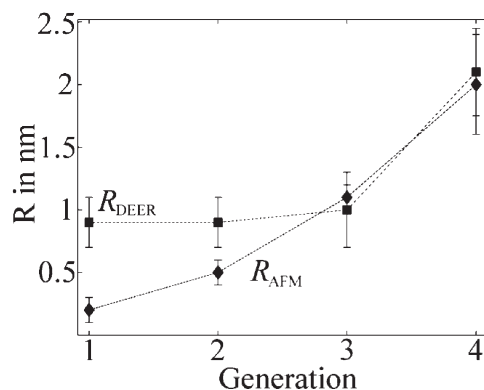


Figure 3. Radii of the different generations of dendronized polymers determined from solution and solid-state measurements plotted versus denpol generation. Values marked R_{DEER} stem from analysis of the data presented in Figure 2 and are representative for the size of the molecules in solution (■). Values marked R_{AFM} stem from AFM tapping of the protected denpols PG1–4 heights published before and are representative for the size in the solid state (◆). Error bars were calculated by subtracting the measured from the corrected radii. (For details, please see the Supporting Information.)

the approximate thickness of the nanoscopic objects. Note that for size-diameter determination it is not necessary for the surface of the denpols to be completely covered with FS ions. With a minimal concentration of positive charges of 28.8 mM (de-PG4) and 4 mM negative charges of FS in the solution, at maximum, 13.8% of the denpol charges could be neutralized, if all FS formed tight ion pairs with the denpol charges. However, as can be seen from the CW EPR spectra (Figure S1 of the Supporting Information), contact of FS with the surface denpol is transient, and only a fraction of FS is bound (with the formation of FS bridges between denpol strands as mentioned above) to the denpol surface at any given moment; no effects on conformation are expected because of charge neutralization. In all cases studied here, a statistical distribution and hence a detectable mean value of distances between spin probes in every direction on the surface is enough to extrapolate and extract the size information, as explained above. The denpol radii so obtained are graphically depicted in Figure 3 and listed in Table 1 together with the radii determined on the basis of the AFM tapping heights (R_{AFM}) determined for the denpols with protected terminal amines on mica.^{1b} The latter can be considered to correspond to the radii of the neutral denpol-analogues in the solid state because the samples are dried on a mica surface during the preparation process. Some phenomena that might influence data gained through AFM and DEER should be noted: (1) AFM is known to underestimate heights of objects on surfaces and (2) DEER measurements are based on electrostatic self-assembly of FS, and hence one has to take into account that not all of the spin probes are fixed to the surface of the cylinders. Thermal motion leads to a radial distribution of spin-probes in the electrostatic potential around the cylinder.¹² Therefore, the radii of the denpols as determined from the DEER time-traces are expected to be shifted to larger values. We correct for these effects by determining the distance distribution of the FS anions at the surface of the polycations. (See Section D in the Supporting Information.) This correction is based on the nonlinear Poisson–Boltzmann equation. The corrected radii so obtained are summarized in Table 1. The distribution functions in Figure 2 are plotted as a function of the unscaled radii.

Note that the minimal detectable distance r_{\min} depends on the pulse length τ_p . For $\tau_p = 12$ ns, $r_{\min} \approx 1.6$ nm (uncorrected) can be estimated,¹⁹ which is in quite good agreement with previous experimental findings²⁰ and the lower distance bound determined by the cylinder model, presented in this study ($R_{\text{DEER}} = 0.8$ nm, which corresponds to a distance of 1.6 nm). The limited excitation bandwidth of the DEER pump pulse precludes the detection of short distances between two spins. This explains why R_{DEER} appears to be equal for generations one and two, although the modulation depth differs significantly. Self-back-folding and 3D network formation has been reported for charged dendronized polymers,²¹ which could lead to aberrations of R_{DEER} from the actual solution radius of the molecules. However, no indications for such phenomena were found during our investigations because fitting the data to bimodal distributions always yielded results similar to fitting with only one distribution. These cautioning words notwithstanding, we expect R_{DEER} to represent a good approximation of the actual radii of the dendronized polymers in solution. Indeed, our data are in good agreement with independent studies.^{1b}

To test further the reliability of the model used, we also measured DEER on mixtures of de-PG2 and de-PG4. The data were fitted with a bimodal distribution based on two cylinders. The time-trace is shown in Figure 2a; the distance distribution is shown red in Figure 2b. The (uncorrected) radius obtained for de-PG2 is 1.2 and for de-PG4 2.4. These values are in good agreement with the radii determined individually from the samples containing a single type of denpol. The mixture contained equal masses of both of the denpols, which leads to 45% of the ammonium-groups present in the system belonging to de-PG4 and 55% to de-PG2. The ratio between the distributions necessary for fitting the data was 0.44, meaning 44% of the distribution in Figure 2b can be traced back to FS on the surface of de-PG2, whereas 56% stem from FS on de-PG4. Taking into account that because of its lower surface charge density the de-PG2-FS attraction is weaker than that between de-PG4-FS, the experimental fractions are in good agreement with the physical picture. We are therefore convinced that a cylindrical shell model is appropriate for analyzing the distribution of molecules on the surface of dendronized polymers and for determining the radius of a particular denpol generation.

Both, R_{DEER} and R_{AFM} increase with increasing generation (cf. Table 1 and Figure 3). The solution radius of the generation 1 and 2 denpols falls short of the corresponding solid state radii. This is attributed to the insensitivity of DEER for low distances, as outlined above. Furthermore, the exceptionally small solid-state (AFM-derived) radius of only 0.2 nm for PG1 might indicate some significant deswelling or contraction on mica. For generations three and four, $R_{\text{DEER}}/R_{\text{AFM}}$ approaches unity; that is, the radius in solution approaches that of the solid state. This finding suggests that highly derivatized and branched denpols in solution may be described as molecular objects. Whereas the term molecular object has been discussed in the context of the protected generation 5 denpol, our data substantiate that even (at least) de-PG3 and de-PG4 fulfill the requirements of this concept. Apparently, steric repulsion between monomer units inhibits a change in structure upon phase transition (from solution to solid state). For low-generation numbers, our data cannot be reliably interpreted because of the excluded distance range below ~ 1.6 nm. One may nonetheless speculate that the low-generation denpols collapse into tightly packed structures upon deswelling and transition from solution state to the solid state. For the high

generations, a collapse seems not to be possible because of repulsive forces between the highly branched monomer units, and the radius remains more or less constant.

In conclusion, DEER is a fast and precise method to determine the size of nanoscopic objects in solution. Here we have developed a simple geometrical model to determine indirectly the thickness of a cylindrical nanosized object in solution. By analysis of the distribution of spin probes self-assembled in the electrostatic potential of the surface of the object, it manifests the idea of dendronized polymers (even as low as generation three) as molecular objects with an environment-independent, persistent shape. In particular, it turned out that the size of the ammonium-terminated denpols in solution becomes similar to the size in the solid state as the generation grows. In the special case with ammonium-terminated denpols addressed here, Freymy's salt as negatively charged spin probe could fortuitously be applied. A correction accounting for the thermal motion of the probe in the electrostatic potential is necessary though. Also, spin labeling of the periphery of a molecular object still remains an option, although this approach may be comparably cumbersome with respect to both time and costs. In addition, it is subject to the risk that the shape of the molecular object is actually changed by the probe or its linker.

Finally, our site-directed spin probing approach to determine sizes of macromolecules with EPR methods may be expanded to all kinds of complex, self-assembled, supramolecular systems because, for example, the attraction of spin-probes to large macromolecules due to hydrophobicity/hydrophilicity is well-documented.²²

■ ASSOCIATED CONTENT

S Supporting Information. CW EPR spectra, molecular structures, HYSCORE spectra, experimental, derivation of distance distributions of particles on a cylinder, and correction of cylinder radii. This material is available free of charge via the Internet <http://pubs.acs.org>.

■ AUTHOR INFORMATION

Corresponding Author

*E-mail: dariush.hinderberger@mpip-mainz.mpg.de.

Author Contributions

[§]These authors contributed equally to this work.

■ ACKNOWLEDGMENT

We thank Christian Bauer for technical support and Prof. Hans W. Spiess for continuing support. D.K. acknowledges support by the Gutenberg Academy of the University of Mainz. This work was financially supported by the Deutsche Forschungsgemeinschaft (DFG) under grant number HI 1094/2-1 and the Max Planck Graduate Center with the University of Mainz (MPGC).

■ REFERENCES

- (1) (a) Stupp, S. I.; Son, S.; Li, L. S.; Lin, H. C.; Keser, M. Bulk Synthesis of Two-Dimensional Polymers: The Molecular Recognition Approach. *J. Am. Chem. Soc.* **1995**, *117*, 5212–5227. (b) Zhang, B.; Wepf, R.; Fischer, K.; Schmidt, M.; Besse, S.; Lindner, P.; King, B. T.; Sigel, R.; Schurtenberger, P.; Talmon, Y.; et al. The Largest Synthetic Structure

with Molecular Precision: Towards a Molecular Object. *Angew. Chem., Int. Ed.* **2011**, *50*, 737–740.

(2) Junk, M. J. N.; Spiess, H. W.; Hinderberger, D. The Distribution of Fatty Acids Reveals the Functional Structure of Human Serum Albumin. *Angew. Chem., Int. Ed.* **2010**, *49*, 8755–8759.

(3) (a) Guo, Y.; Beek, J. D. v.; Zhang, B.; Colussi, M.; Walde, P.; Zhang, A.; Kröger, M.; Halperin, A.; Schlüter, A. D. Tuning Polymer Thickness: Synthesis and Scaling Theory of Homologous Series of Dendronized Polymers. *J. Am. Chem. Soc.* **2009**, *131*, 11841–11854. (b) Schlüter, A. D.; Rabe, J. P. *Angew. Chem., Int. Ed.* **2000**, *39*, 864–883.

(4) (a) Shu, L.; Schlüter, A. D. Synthesis and Polymerization of an Amine-Terminated Dendronized Styrene. *Macromolecules* **2000**, *201*, 239–245. (b) Li, W.; Wu, D.; Schlüter, A. D.; Zhang, A. Synthesis of an Oligo(ethylene glycol)-Based Third-Generation Thermoresponsive Dendronized Polymer. *J. Polym. Sci., Part A* **2009**, *47*, 6630–6640.

(5) Shu, L.; Schäfer, A.; Schlüter, A. D. Dendronized Polymers: Increasing of Dendron Generation by the Attach-to Approach. *Macromolecules* **2000**, *33*, 4321–4328.

(6) Schweiger, A.; Jeschke, G. *Principles of Pulse Electron Paramagnetic Resonance*; Oxford University Press: New York, 2001.

(7) (a) Jeschke, G.; Sajid, M.; Schulte, M.; Ramezani, N.; Volkov, A.; Zimmermann, H.; Godt, A. Flexibility of Shape-Persistent Molecular Building Blocks Composed of *p*-Phenylene and Ethynylene Units. *J. Am. Chem. Soc.* **2010**, *132*, 10107–10117. (b) Pornsuwan, S.; Bird, G.; Schafmeister, C. E.; Saxena, S. Flexibility and Lengths of Bis-Peptide Nanostructures by Electron Spin Resonance. *J. Am. Chem. Soc.* **2006**, *128*, 3876–3877. (c) Godt, A.; Schulte, M.; Zimmermann, H.; Jeschke, G. How Flexible Are Poly(paraphenyleneethynylene)s? *Angew. Chem., Int. Ed.* **2006**, *45*, 7722–7726. (d) Margraf, D.; Bode, B. E.; Marko, A.; Schiemann, O.; Prisner, T. F. Conformational Flexibility of Nitroxide Biradicals Determined by X-band PELDOR Experiments. *Mol. Phys.* **2007**, *105*, 2153–2160. (e) Lovett, J. E.; Hoffmann, M.; Cnossen, A.; Shutter, A. T. J.; Hogben, H. J.; Warren, J. E.; Pascu, S. I.; Kay, C. W. M.; Timmel, C. R.; Anderson, H. L. Probing Flexibility in Porphyrin-Based Molecular Wires Using Double Electron–Electron Resonance. *J. Am. Chem. Soc.* **2009**, *131*, 13852–13859.

(8) (a) Bird, G. H.; Pornsuwan, S.; Saxena, S.; Schafmeister, C. E. Distance Distributions of End-Labeled Curved Bispeptide Oligomers by Electron Spin Resonance. *ACS Nano* **2008**, *2*, 1857–1864. (b) Schiemann, O.; Cekan, P.; Margraf, D.; Prisner, T. F.; Sigurdsson, S. T. Relative Orientation of Rigid Nitroxides by PELDOR: Beyond Distance Measurements in Nucleic Acid. *Angew. Chem., Int. Ed.* **2009**, *48*, 3292–3295.

(9) Hinderberger, D.; Spiess, H. W.; Jeschke, G. Dynamics, Site Binding, and Distribution of Counterions in Polyelectrolyte Solutions studied by EPR Spectroscopy. *J. Phys. Chem. B* **2004**, *108*, 3698–3704.

(10) Höfer, P.; Grupp, A.; Mehring, M. Hyperfine Sublevel Correlation (HYSCORE) Spectroscopy: A 2D ESR Investigation of the Squaric Acid Radical. *Chem. Phys. Lett.* **1986**, *132*, 279–282.

(11) Kurzbach, D.; Sharma, A.; Sebastiani, D.; Klinkhammer, K. W.; Hinderberger, D. Dinitrogen Complexation With Main Group Radicals. *Chem. Sci.* **2011**, *2*, 473–479.

(12) Hinderberger, D.; Spiess, H. W.; Jeschke, G. Radial Counterion Distributions in Polyelectrolyte Solutions Determined by EPR Spectroscopy. *Europhys. Lett.* **2005**, *70*, 102–108.

(13) We stick to the notation introduced by Schlüter and coworkers. Therefore, de-PG denotes deprotected, terminal ammonium groups.

(14) (a) Schmidt-Rohr, K.; Rawal, A.; Fang, X.-W. A New NMR Method for Determining the Particle Thickness in Nanocomposites, Using T_{2H} -Selective $X\{^1H\}$ Recoupling. *J. Chem. Phys.* **2007**, *126*, 054701-1–054701-16. (b) Borbat, P. P.; Davis, J. H.; Butcher, S. E.; Freed, J. H. Measurement of Large Distances in Biomolecules Using Double-Quantum Filtered Refocused Electron Spin-Echoes. *J. Am. Chem. Soc.* **2004**, *126*, 7746–7747.

(15) Jeschke, G.; Chechik, V.; Ionita, P.; Godt, A.; Zimmermann, H.; Banham, J.; Timmel, C. R.; Hilger, D.; Jung, H. DeerAnalysis2006 - A Comprehensive Software Package for Analyzing Pulsed ELDOR Data. *Appl. Magn. Reson.* **2006**, *30*, 473–498.

(16) Jeschke, G.; Sajid, M.; Schulte, M.; Godt, A. Three-Spin Correlations in Double Electron–Electron Resonance. *Phys. Chem. Chem. Phys.* **2009**, *11*, 6580–6591.

(17) Jeschke, G.; Koch, A.; Jonas, U.; Godt, A. Direct Conversion of EPR Dipolar Time Evolution Data to Distance Distributions. *J. Magn. Reson.* **2002**, *155*, 72–82.

(18) Fajer, P. G.; Brown, L.; Song, L., Practical Pulsed Dipolar ESR (DEER). In *ESR Spectroscopy in Membrane Biophysics*; Hemminga, M. A., Berliner, L. J., Eds.; Springer: New York, 2007.

(19) Tsvetkov, Y. D.; Milov, A. D.; Maryasov, A. G. Pulsed Electron–electron Double Resonance (PELDOR) as EPR Spectroscopy in Nanometre Range. *Russ. Chem. Rev.* **2008**, *77*, 487–520.

(20) Banham, J. E.; Baker, C. M.; Ceola, S.; Day, I. J.; Grant, G. H.; Groenen, E. J. J.; Rodgers, C. T.; Jeschke, G.; Timmel, C. R. Distance Measurements in the Borderline Region of Applicability of CW EPR and DEER: a Model Study on a Homologous Series of Spin-Labelled Peptides. *J. Magn. Reson.* **2008**, *191*, 202–218.

(21) Zhuang, W.; Kasemi, E.; Ding, Y.; Kröger, M.; Schlüter, A. D.; Rabe, J. P. Self-Folding of Charged Single Dendronized Polymers. *Adv. Mater.* **2008**, *20*, 3204–3210.

(22) (a) Junk, M. J. N.; Jonas, U.; Hinderberger, D. EPR Spectroscopy Reveals Nanoinhomogeneities in the Structure and Reactivity of Thermoresponsive Hydrogels. *Small* **2008**, *4*, 1485–1493. (b) Junk, M. J. N.; Li, W.; Schlüter, A. D.; Wegner, G.; Spiess, H. W.; Zhang, A.; Hinderberger, D. EPR Spectroscopic Characterization of Local Nanoscopic Heterogeneities during the Thermal Collapse of Thermoresponsive Dendronized Polymers. *Angew. Chem., Int. Ed.* **2010**, *122*, 5818. *Angew. Chem., Int. Ed.* **2010**, *49*, 5683.